DOI 10.1002/prca.200600802 *Proteomics Clin. Appl.* 2007, *1,* 494–505

RESEARCH ARTICLE

An experimental strategy for quantitative analysis of the humoral immune response to prostate cancer antigens using natural protein microarrays

Sara Forrester[1], Ji Qiu[2], Leslie Mangold[3], Alan Partin[3], David Misek[4], Brett Phinney[5], Douglas Whitten[5], Philip Andrews[4], Eleftherios Diamandis[6], Gilbert S. Omenn[4], Samir Hanash[2] and Brian B. Haab[1]*

[1] Van Andel Research Institute, Grand Rapids, MI, USA
[2] Fred Hutchinson Cancer Research Center, Seattle, WA, USA
[3] John Hopkins University School of Medicine, Baltimore, MD, USA
[4] University of Michigan Medical School, Ann Arbor, MI, USA
[5] Michigan State University, East Lansing, MI, USA
[6] University of Toronto, Toronto, Ontario, Canada

Received: October 19, 2006
Revised: February 1, 2007
Accepted: February 23, 2007

The identification of human tumor antigens has potential utility in the diagnosis and treatment of cancers. We demonstrate here a complete strategy to profile immunoreactivity and identify tumor antigens from proteins derived from tumor cell lines. Microarrays of proteins produced from 2-D LC fractionation of prostate tumor cell-line lysates were used to profile immunoreactivity in the sera of prostate cancer patients and control subjects. Cancer-associated immunoreactivity to distinct groups of chromatography fractions was present in about 50% of the patients, with greater immunoreactivity present in patients with non-organ-confined cancer than in patients with organ-confined cancer. We grouped the immunoreactive fractions by similarities in elution order and patterns of immunoreactivity to guide and interpret the MS analysis of selected fractions, which was used to identify the proteins that may be responsible for the immunoreactivity. As a complementary method to further characterize and validate the immunoreactivity of the proteins identified by mass spectrometry, we demonstrate the use of focused microarrays of recombinant proteins. Disease-associated immunoreactivity was confirmed for one of the identified proteins, human Kallikrein 11. These results demonstrate a practical approach to screening, identifying, and validating immunoreactive proteins that could be applied to diverse studies on humoral immune responses.

Keywords:
Humoral immune response / Prostate cancer / Protein arrays

Correspondence: Dr. Brian B. Haab, Van Andel Research Institute, 333 Bostwick, Grand Rapids, MI 49503, USA
E-mail: Brian.Haab@vai.org
Fax: +1-616-234-5269

Abbreviations: **hK11,** human Kallikrein 11; **PBST0.1,** PBS with 0.1% Tween 20; **PBST0.5,** PBS with 0.5% Tween 20; **PSA,** prostate-specific antigen

1 Introduction

It has long been known that many types of cancers commonly elicit an immune response. A better understanding of the biological significance of the immune response, its use in

* Present address: University of California Davis Genome Center, Genome Biomedical Sciences Facility, Davis, CA, USA

diagnosing or classifying cancers, and its potential therapeutic use in treating cancers could be beneficial for cancer patients. Knowledge of the specific tumor-associated antigens and of the immune responses against those antigens is critical for eventual research or clinical uses of the immune response. Recently, we and other groups have demonstrated that natural protein microarrays, in which the arrays are spotted with multi-dimensional, liquid-based fractions of proteins from native sources such as human cells and tissues, can be a valuable screening tool for the discovery of tumor-associated antigens [1, 2]. This report presents a robust strategy for immune profiling using natural proteins in arrays, combined with identification and validation of antigens in those protein fractions.

The natural protein microarray method is complementary to other strategies that have been developed for discovering tumor antigens. Serological analysis of cDNA expression libraries (SEREX) [3, 4] involves the construction of a cDNA library from tumor tissue, expression in a phage system, and panning against sera from cancer patients. This method has been used to identify many tumor antigens [3, 5, 6]. In a recent report, microarrays of selected members of fusion-peptide libraries were used to discover multiple autoantibodies associated with prostate cancers [7]. An advantageous feature of natural protein arrays is that proteins are taken from their native states, so that potentially immunogenic and biologically significant alterations to the proteins may be detectable. Another method that uses proteins taken from native states is 2-DE separations of tumor cell material followed by Western blot analysis using patient sera. That method has led to the identification of tumor antigens in pancreatic [8], lung [9, 10], breast [11], colon [12], hepatocellular [13], and ovarian cancers [14]. Advantages of natural protein arrays over gel blots are higher reproducibility, wider range of proteins detected, simplified data interpretation, and higher throughput.

Prostate cancer is an immunogenic tumor, as shown by the identification of antibodies against many tumor-associated antigens in prostate tumors. For example, antibodies have been detected in serum or plasma of prostate cancer patients against proteins such as alpha-methyl-acyl-CoA racemase (AMACR) [15], enhancer of zeste homolog 2 (EZH2) [16], PSA [17], HER-2/neu [17], secretory granules of the prostate [18], and lens epithelium-derived growth factor p75 (LEDGF/p75) [19]. The high prevalence of a tumor-associated immune response in patients with prostate cancers was shown in a study of a panel of six tumor-associated antigens [20] with a positive response in cancers at 92.5% *vs.* 14.8% in normals, as well as with microarrays of phage-displayed polypeptides at a specificity of 88.2% and 81.6% sensitivity [7].

A practical strategy to profile the autoantibody reactivity from prostate cancer patients against multiple cancer-derived proteins could better harness information from the immune response for benefit to patients. The identification of new tumor antigens from tumor-derived or cell-line-derived material could lead to the development of effective diagnostic tests or the better understanding of protein alterations in the tumor environment. We report here such a strategy using natural protein arrays derived from a prostate cancer cell line, combined with improvements to identify some of the immunoreactive proteins, with an example of confirming such identification for one protein using a focused microarray.

2 Materials and methods

2.1 Serum samples

Serum samples were collected as part of a HIPAA-compliant, IRB-approved, National Cancer Institute-sponsored protocol (through the Early Detection Research Network) at the Johns Hopkins Medical Institution. Samples were collected prior to a prostate biopsy or prostatectomy that had been dictated by an elevated prostate-specific antigen (PSA) concentration (>4.0 ng/mL) and/or an abnormal digital rectal examination (DRE). Patients with biopsy-confirmed cancer underwent radical retropubic prostatectomy. The tumors were mostly Gleason grade 6 or 7. The cancers were classified as organ-confined or non-organ-confined based on the surgical pathology. The cancers in the non-organ-confined class had capsular penetration and, in a few cases, lymph node and seminal vesicle involvement. Control sera were collected from age-similar men with normal serum PSA levels and a negative DRE as part of a routine community-screening program. The demographic information from the control group was statistically similar to the patient groups. A summary of the sample numbers, age of patients, and PSA values of the samples is given in Table 1. The samples were stored frozen at −80°C and shipped frozen on dry ice to the Van Andel Research Institute.

2.2 Cell culture and protein extraction

The LNCaP cell line (ATCC, Manassas, VA), which is a metastatic prostate cancer cell line, was cultured in RPMI 1650 medium supplemented with 10% FCS (Invitrogen, Carlsbad, CA). Approximately 50 mg of protein was extracted by solubilizing the cells in a lysis buffer of 6 M urea, 2 M thiourea, 1.0% n-octyl beta-D-glucopyranoside, 2 mM dithioerythritol, protease inhibitor cocktail (Roche, Basel, Switzerland), and 2% carrier ampholytes, pH 3.5–10 (Bio-Rad, Hercules, CA). We collected protein from 12 P100 culture dishes containing approximately 9.5×10^6 cells/plate, resulting in approximately 50 mg of protein. The protein extract was stored at −80°C until ready for use.

2.3 Protein fractionation

The cell lysates were fractionated by 2-D LC. The first dimension of separation was liquid phase IEF using a preparative scale Rotofor (Bio-Rad) to collect 20 fractions, start-

Table 1. Samples used in the experiments

Profiling experiments (sets 1, 2, and 3)			
Class	Number	Age (SD)	PSA (SD)
Healthy control	46	55 (6.5)	0.7 ng/mL (0.48)
Non-organ-confined prostate cancer	51	60 (6.5)	6.3 ng/mL (5.74)
Organ-confined prostate cancer	50	57 (6.4)	5.2 ng/mL (2.49)
Focused arrays			
Class	Number	Age (SD)	PSA (SD)
Healthy control	66	54 (6.4)	0.7 ng/mL (0.52)
Non-organ-confined prostate cancer	69	60 (6.4)	6.5 ng/mL (5.28)
Organ-confined prostate cancer	70	57 (6.4)	5.1 ng/mL (2.46)

ing from 50 mg of protein. Each of the fractions was further separated by RP-HPLC in the second dimension. Separations were performed on an R2/20 RP column (Applied Biosystems, Foster City, CA) using a gradient of water and ACN (buffer A: 98% H_2O/2% ACN/0.1% TFA; buffer B: 10% H_2O/90% ACN/0.1% TFA) at a flow rate of 3 mL/min. The gradient profile used was as follows: (i) 90% A to 80% A in 2.5 min; (ii) 80% A to 30% in 55 min; (iii) 30% A to 0% A in 2.5 min. Eighty-four RP fractions were collected for each of the 20 first-dimension fractions. The resulting 1680 fractions were collected into 20 96-well microtiter plates (1 plate for each of the first-dimension collections) and lyophilized to dryness. Each fraction was resuspended in 35 μL PBS (137 mM NaCl; 2.7 mM KCl; 10.1 mM Na_2HPO_4; 1.8 mM KH_2PO_4). An estimated average of 3.5 μg of protein was collected in each fraction, resulting in a 100 μg/mL average protein concentration in the resuspensions.

2.4 Microarray production and use

The resuspended 1680 fractions and controls [PBS, anti-human IgG (biotinylated and not), anti-IgM, anti-Albumin, PSA, and Tetanus Toxoid] were printed in duplicate spots on NC-coated slides (Schleicher and Schuell, Keene, NH) using a custom-built contact printer that was an enhanced version of an earlier contact printer design [21]. The microarrays were printed in three successive batches, with each batch used for a separate experiment set. After printing, the slides were stored vacuum-sealed with desiccant at 4°C until use.

Each array was circumscribed with a border that was applied by hand using a hydrophobic marker (Super HT Pap Pen, Scientific Devices Laboratory, Des Plaines, IL). The arrays were rinsed for 30 s in PBS with 0.5% Tween 20 (PBST0.5) then washed three times with gentle rocking for 3 min in fresh changes of PBST0.5. The slides were blocked in 1% BSA in PBST0.5 for 2 h at room temperature with gentle shaking. Each serum sample was diluted 1:60 in PBST0.1. In the first two experiment sets, the diluent contained 2 μg/mL dinitrophenol-labeled BSA (labeled using N-hydroxysuccinimide-DNP, Invitrogen) and 1 μg/mL flag-labeled bacterial alkaline phosphatase (Sigma) as controls. Three hundred microliters of each diluted serum solution was incubated on an array for 90 min at room temperature with gentle shaking. The arrays were rinsed and washed three times, 5 min each, in PBST0.1. Biotinylated anti-human Ig (Amersham Biosciences) (5 μg/mL) in 3% nonfat milk/PBST0.1 was incubated on the arrays for 1 h with gentle shaking followed by three 5-min washes with PBST0.1. Streptavidin-phycoerythrin (Amersham Biosciences) (10 μg/mL) in 3% nonfat milk/PBST0.1 was incubated on each array for 1 h with gentle shaking. The microarrays were washed three times, 5 min each, with PBST0.1 and dried by centrifugation at $150 \times g$ for 3 min.

The microarrays were scanned for fluorescence with a microarray scanner (ScanArray, Perkin Elmer Life Sciences, Boston, MA) using a green laser (543 nm) set to consistent detector gain and laser power settings for all slides. The images were analyzed using the GenePix Pro 5.0 (Axon Instruments) software program. The background-subtracted intensities of duplicate spots were averaged using the geometric mean. Hierarchical clustering and visualization were performed using the Cluster and Treeview programs (see http://rana.lbl.gov/). The M2 statistics [22] was calculated in Microsoft Excel. For each fraction, the M2 score was the number of samples within a patient group that had intensity above a threshold, defined as the second-highest intensity in a control group of samples.

2.5 MS

Prior to analysis by MS, the proteins in the fractions to be analyzed were digested in a 1/10 volume of ACN and 1 μL of MS grade Trypsin Gold (Promega) at a concentration of 20 ng/mL. The digested fractions were stored at –80°C until analysis. Two MS methods were used to analyze the digested proteins.

At the Michigan State University Proteomics Facility (http://www.proteomics.msu.edu/), the digested fractions were analyzed by nano-scale LC/MS/MS using a Surveyor HPLC system connected to a Linear Ion Trap Quadrupole Fourier Transform (LTQ-FT, Thermo Electron). The digested peptides were trapped on a homemade 100 μm × 5 mm nano-trap packed with Magic C18AQ 5 μm packing material (Michrom Bioresources). After the peptides were trapped, they were eluted with a gradient of 2%B to 40%B in 25 min (40 min total analysis time *per* sample) (A = 0.1% formic acid, B = 100% ACN, 0.1% formic acid) on a 75 μm × 100 mm picofrit column (New Objectives) packed with Magic C18AQ. Mass spectra were acquired with the following instrument parameters: the top eight ions were isolated and analyzed with the FT detector (1–2 ppm accuracies) while simultaneously being fragmented in the LTQ to obtain MS/MS data (200–400 ppm accuracies). Peak lists

were extracted using "extract_msn" and searched using the X!Tandem search algorithm (Beavisinformatics). Identifications were considered correct if the protein score had a probability score of −3.0 or below. False positive identification rates were determined by reversing the ensemble human database and using X!Tandem modified Probit algorithm built into X!Tandem. Estimated false positives and reversed sequence false positives were zero when the minimum protein log(e) score was −3.0 or below. Proteins with fewer than two peptides identified were verified using the verification tool on the global proteome machine (www.thegpm.org).

At the Proteome Mapping Core at the University of Michigan (http://www.proteomeconsortium.org/), the trypsin-digested protein fractions were subjected to RP capillary HPLC on an Agilent 1100 instrument using a Zorbax SB-C18, 150 × 0.1 mm column at a flow rate of 400 nL/min. In total, 224 fractions were collected on a MALDI plate using an Agilent MALDI fraction collector with online addition of CHCA (2 mg/mL containing 10 mM ammonium phosphate in 50% isopropanol, 1% acetic acid). Plates were subjected to MS/MS analysis on an Applied Biosystems model 4700 MALDI TOF-TOF MS/MS spectrometer. Acquisition of data was under 4000 series Explorer software using results-dependent acquisition with MS/MS run on ions at their peak intensities. The peak lists were searched through the NCBInr human sequence database using GPS 3.0 (MASCOT v1.9-based). Consolidations of protein identifications were performed manually.

2.6 Focused protein microarrays

Recombinant human Kallikrein 11 (hK11) isoform 1 protein was purchased (R&D Systems, 1595-SE), and recombinant hK11 isoform 2 protein and anti-hK11 polyclonal antibody were obtained from the laboratory of Dr. Elephtherios Diamandis at the University of Toronto. The proteins were prepared at 0.5 mg/mL in PBS and were assembled in a polypropylene 384-well microtiter plate (MJ Research), along with the proteins BSA, human IgM, human IgG, alpha-1-antitrypsin, C-reactive protein, PSA, IGF-2, and carcinoembryonic antigen. A piezoelectric non-contact printer (Biochip Arrayer, Perkin Elmer) spotted approximately 350 p*l* of each protein solution on the surfaces of ultra-thin-NC-coated microscope slides (PATH slides, GenTel Biosurfaces). Ultra-thin NC was used here instead of thick NC because less binding capacity is needed for purified protein solutions than for the lysate fractions described above. The thin NC is otherwise preferable because it has a lower auto-fluorescent background relative to the thick NC. Forty-eight identical arrays were printed on each slide, with each 1.5 × 1.5 mm individual array consisting of 12 proteins spotted in triplicate. The slides were imprinted with a wax border around each of the arrays to define hydrophobic boundaries, using a custom-built device. This device, described in more detail elsewhere [23], prints wax lines on a slide in precise locations, and its use was necessary in this application since the hand-application of hydrophobic lines using a marker is not precise enough for the small and tightly-spaced arrays used here. The slides were rinsed briefly in PBST0.5, blocked for 1 h at room temperature in PBST0.5 containing 1% BSA, and rinsed two more times with PBST0.5. Slides were dried by centrifugation at 150 × *g* for 3 min prior to sample application. The serum samples were diluted 1:5 into PBST0.1, and 7 μL of each sample was pre-incubated for 1 h at room temperature on a blank PATH slide, which had been blocked in PBST0.5 containing 1% BSA. The pre-incubation of the sample on NC was found to be important in reducing non-specific binding in the experiments. Six microliters of each sample was removed from the preincubation slide and incubated on a protein microarray with gentle rocking at room temperature for 1 h. The slides were then processed as described above.

3 Results

3.1 Profiling tumor immunoreactivity using microarrays of tumor-derived proteins

Three sets of experiments were performed to probe for the presence of tumor-reactive antibodies in the sera of prostate cancer patients and controls. The first two were duplicates of each other, using serum samples from patients with non-organ-confined prostate cancer ($n = 51$) and from healthy subjects ($n = 46$); the third used serum samples from patients with organ-confined prostate cancer ($n = 50$) and from the same healthy subjects ($n = 46$) (Table 1). Each of the three experiment sets used a distinct batch of microarrays, each batch printed on a different day. Each serum sample was incubated on an array containing the fractions of a 2-D separation of tumor-cell-line proteins, and the amount of Ig binding to each fraction was quantified.

The overall reproducibility of the assay was examined by comparing the results from the duplicate experiment sets (one and two). A correlation coefficient (r) was calculated between the data from each array in experiment set one and the corresponding array (incubated with the same sample) in experiment set two (excluding data from the control spots). Fifty-seven of the 100 arrays had correlations of over 0.9 between the experiment sets, and all but two had correlations over 0.8, showing a high level of reproducibility (Supporting Fig. 1A). Correlation coefficients also were calculated between each fraction in experiment set one and the corresponding fraction in experiment set two for the data over all the samples. The correlations in this case averaged around 0.7, with a range of 0.1–0.99 (Supporting Fig. 1B). The lower average correlations for the fractions are due to the fact that some fractions showed very little antibody binding. Negative control arrays, in which PBS buffer was incubated instead of serum, showed no anti-human-Ig binding (Supporting Fig. 2).

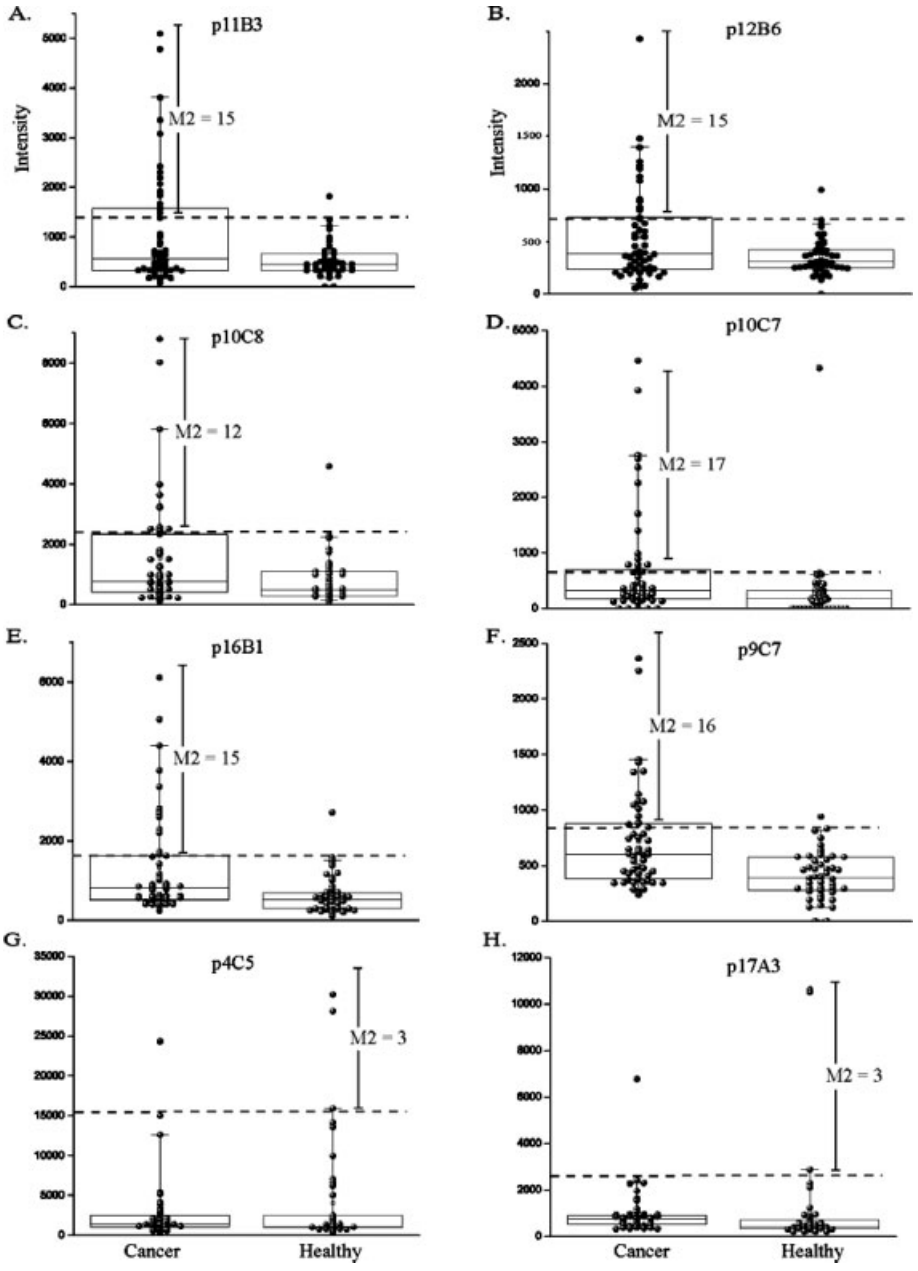

Figure 1. Scatter and box plots of signal intensities. The intensities of antibody binding to the indicated fractions is shown for the cancer samples (left in each plot) and the control samples (right in each plot), in which each point is an individual sample. The box in each plot indicates the upper and lower quartiles, with the line in the box indicating the median value. Panels (A–C) present data from non-organ-confined cancer patients, and panels (D–F) present data from organ-confined cancer patients. The dashed line in panels (A–F) indicates the level of the second-highest control sample, and the M2 score indicates the number of cancer samples above that threshold. The dashed line in panels (G) and (H) indicates the level of the second-highest cancer sample, and the M2 score indicates the number of control samples above that threshold. The two fractions with the highest M2 scores calculated in that way are shown.

3.2 Identifying fractions with cancer-associated immunoreactivity

We compared the levels of antibody binding to each of the fractions between the cancer samples and the control samples in order to identify those fractions most likely to contain cancer antigens. Because antibody reactivity is normally present only in a subset of patients, with a non-normal distribution, we used the M2 statistics [22] to pick out the fractions with potential cancer-associated reactivity. For each fraction, a threshold is defined as the second-highest level of reactivity among the control patients. The M2 statistics counts the number of cancer patients above that threshold (Fig. 1). Figure 1 shows the distributions of signal intensities for the fractions with the top three M2 scores for the non-organ-confined (M2 ranging from 12–15) and the organ-confined samples (M2 ranging from 15–17). To get some idea of the M2 scores that would be produced by chance, one may define a threshold as the second-highest cancer sample and count the number of normal samples above that threshold. The M2 scores for the control samples are minimal (top values 3 and 3) and are similar to what would be expected by chance [22]. This analysis shows a higher level of immunoreactivity in the cancer samples as compared to the control

samples for certain fractions. Many other fractions had high M2 scores when counting the number of cancer samples exceeding a threshold defined by the controls samples, as shown by the distributions of M2 scores shown in Supporting Fig. 3. The fact that the results were reproducible in two completely randomized experiment sets, and that the cancer-associated immunoreactivity was observed in only a subset of the fractions, strongly suggest that these results were not the result of systematic bias in the data.

3.3 Defining groups of fractions containing common immunoreactive proteins

Having identified individual fractions that may contain tumor antigens, our next goal was to develop a method to define the groups of fractions that may contain common immunoreactive proteins. Because the 2-D LC separation does not completely resolve the component proteins of a cell lysate, each protein may be eluted in multiple, sequential fractions. A method to identify groups of fractions that contain the same immunoreactive protein could help to guide the further analysis of those fractions and the identification of the immunoreactive proteins. Two pieces of information were used to define which fractions contain a common immunoreactive protein. One was the order of the elution of the fractions, and the other was the pattern of reactivity over the samples. Fractions that share a common immunoreactive protein should have eluted in adjacent chromatography fractions, and they should share the same pattern of reactivity over all the samples.

To visualize how the immunoreactive fractions grouped in the chromatography order, the M2 scores of all the fractions were arranged by order of separation, with the horizontal axis representing the IEF dimension and the vertical axis representing the RP chromatography dimension (Fig. 2). Clusters of high M2 scores appear for both the non-organ-confined (A) and the organ-confined samples (B). The observation of clusters of reactivity is consistent with the elution of immunoreactive proteins over several adjacent fractions. About seven clusters of highly reactive fractions

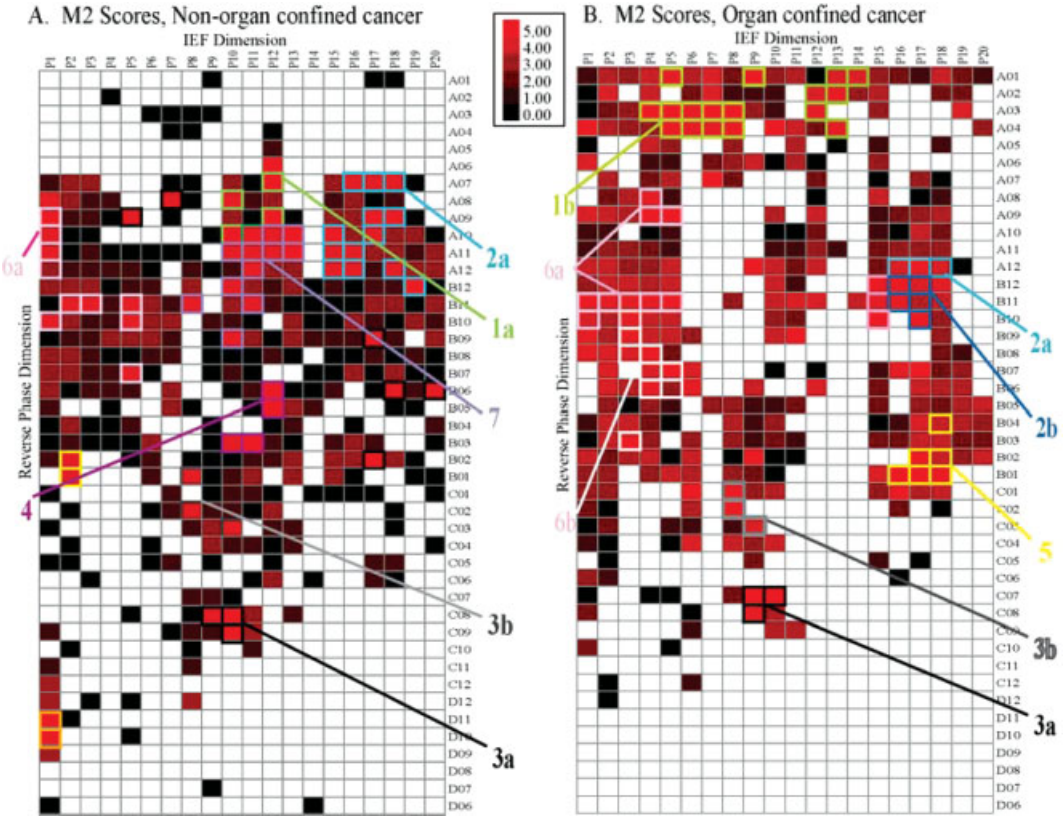

Figure 2. Locations of M2 scores in the fractionation. Each box represents a chromatography fraction, with all the boxes arranged by elution order. The 20 columns represent the IEF first dimension, and the 84 rows represent the RP-HPLC second dimension. The intensity of each box indicates the M2 score of each fraction (indicated by the color bar, log base 2). The colored outlines show the 60 fractions with the highest M2 scores in each fraction, which are also colored and labeled by clustered groups (also corresponding to the clusters shown in Fig. 3). (A) M2 scores for non-organ-confined cancer relative to controls, counting only samples that passed the threshold in both experiment sets one and two. Only M2 scores above 3 are shown, and the rest are blanked for clarity. (B) M2 scores for organ-confined cancer relative to controls in experiment set three. Only M2 scores above four are shown, and the rest are blanked.

appear in each graph, as defined by the 60 fractions with the highest M2 scores (highlighted in the graphs). Each of the clusters was numbered, with clusters that were common between the organ-confined and non-organ-confined samples given the same number. Immunoreactivity was observed only from fractions obtained in the first half of the RP separations (Figs. 2A and B). The hydrophobic fractions of the second half of the RP elution probably were not soluble in the aqueous resuspension buffer and therefore most likely were not spotted onto the arrays.

Next, we examined the patterns of reactivity of the adjacent fractions. Fractions that contain a common immunoreactive protein should have similar patterns of reactivity over all the samples. The patterns of reactivity over all the samples of the 60 fractions in each experiment set with the highest M2 scores (highlighted in Fig. 2) were visualized by clustering (Fig. 3). The fractions clustered according to location in the fractionation, meaning that fractions close to each other in the fractionation also have similar patterns of reactivity over all the samples. For example, all the fractions of group 5 (yellow) have a similar pattern to each other and a completely different pattern from all the fractions of group 1 (green). Therefore, the fractions within each group likely share common immunoreactive proteins and the different groups contain different immunoreactive proteins. Some groups share similar patterns, such as groups 7, 2a, 6a, and 1a in Fig. 3A, so the same protein may be reactive in these groups. The adjacent fractions had been spotted in distinct regions of the microarrays, so the clustering of reactivities was not due to spatial bias on the arrays.

The clusters gave some indication of the distribution in the amount of total immunoreactivity in the patients. This information is useful to predict how common this immunoreactivity is likely to be in a broader population of cancer patients, and how useful a biomarker based on these antigens might be. About 50% of the patients had reactivity with seven or more of the fractions, whereas only 6% of the controls had the same level of immunoreactivity. Since the patterns of immunoreactivity are distinct between the different groups, a panel of markers based on these different reactivities would perform better than measuring reactivity to any one protein. The actual diagnostic performance will need to be tested using purified proteins, rather than chromatography fractions, and additional samples.

3.4 Identification of proteins in the immunoreactive fractions

The ability to group the fractions according to clusters that each likely contains a common immunoreactive protein guided the selection of fractions for protein identification by MS and the eventual interpretation of the data. We chose several fractions from each of the groups of Fig. 2 (57 fractions total) for analysis by LTQ-FT-MS. Five of the 57 fractions also were analyzed by MALDI-MS/MS to provide information on the depth of protein identification provided by each method. The entire volume of each fraction not used for making microarrays was consumed in the MS/MS analysis (typically 8 μL), in order to optimize the potential for accurate identifications.

There were 1289 high-confidence protein identifications made, with 0 to 66 proteins *per* fraction and 546 unique proteins identified. No correlation was observed between number of proteins identified and location in the fractionation. There were 266 proteins identified in only 1 fraction, 131 were found in 2 fractions, 46 were found in 3 fractions, and the remaining 103 in 4 or more, whereas, 1 protein (nucleolin) was found in 16 fractions. Some proteins were found in many different groups, up to seven different groups, across the entire separation, and others were tightly clustered within one group. For example, the protein tubulin-specific chaperone A was identified in 4 fractions from three different, well-separated groups, but the protein 14-3-3 gamma was found in 5 different fractions that were all within the group 6a. Therefore, it appears that the resolution of the separations was protein dependent. A complete list of all proteins identified is given in Supporting Table 1.

Fractions within the same group usually shared many of the same protein identifications, which would be expected since those fractions were close in the elution order. For example, in the four fractions from group 4 of Fig. 2A (fractions p12b5, p12b6, p10b3, p11b3), 23 to 53 proteins were identified in each fraction by either LTQ-FT-MS or MALDI-MS/MS, and almost all of those were found in at least two of the four fractions, with 11 proteins identified in all four fractions. These observations agreed qualitatively with gel electrophoresis analysis of some of the fractions, which showed the presence of multiple protein bands and similar band patterns between adjacent fractions. Only up to about 15 bands were observable by electrophoresis, showing the higher resolving power and sensitivity of MS (data not shown).

The analysis of five fractions by the two MS methods allowed a comparison of the identified proteins between those methods. In the analysis of three fractions from group 4 (p11B3, p10B3, p12B6), 4 proteins were found only by LTQ-FT-MS, 11 proteins were found only by MALDI-MS/MS, and 22 were found by both techniques. In fraction p3b9, the same single protein, heterogeneous nuclear ribonucleoprotein A2/B1 (HNRPA2B1), was found by each method, and in fraction p4a9, 6 and 8 proteins were found by MALDI-MS/MS and LTQ-FT-MS, respectively, with 2 proteins found in common. Therefore, many proteins were found by both methods, but some unique identifications were obtained. These results emphasize the advantage of using multiple methods to obtain the most comprehensive protein identifications.

The selection of adjacent fractions likely to contain a common immunoreactive protein presented a strategy for narrowing the list of the best candidate antigens. We reasoned that the best candidates would be found in multiple fractions within a single group, not spread out across multiple groups. Poorly resolved proteins, found in multiple groups of the separation, would not produce high and

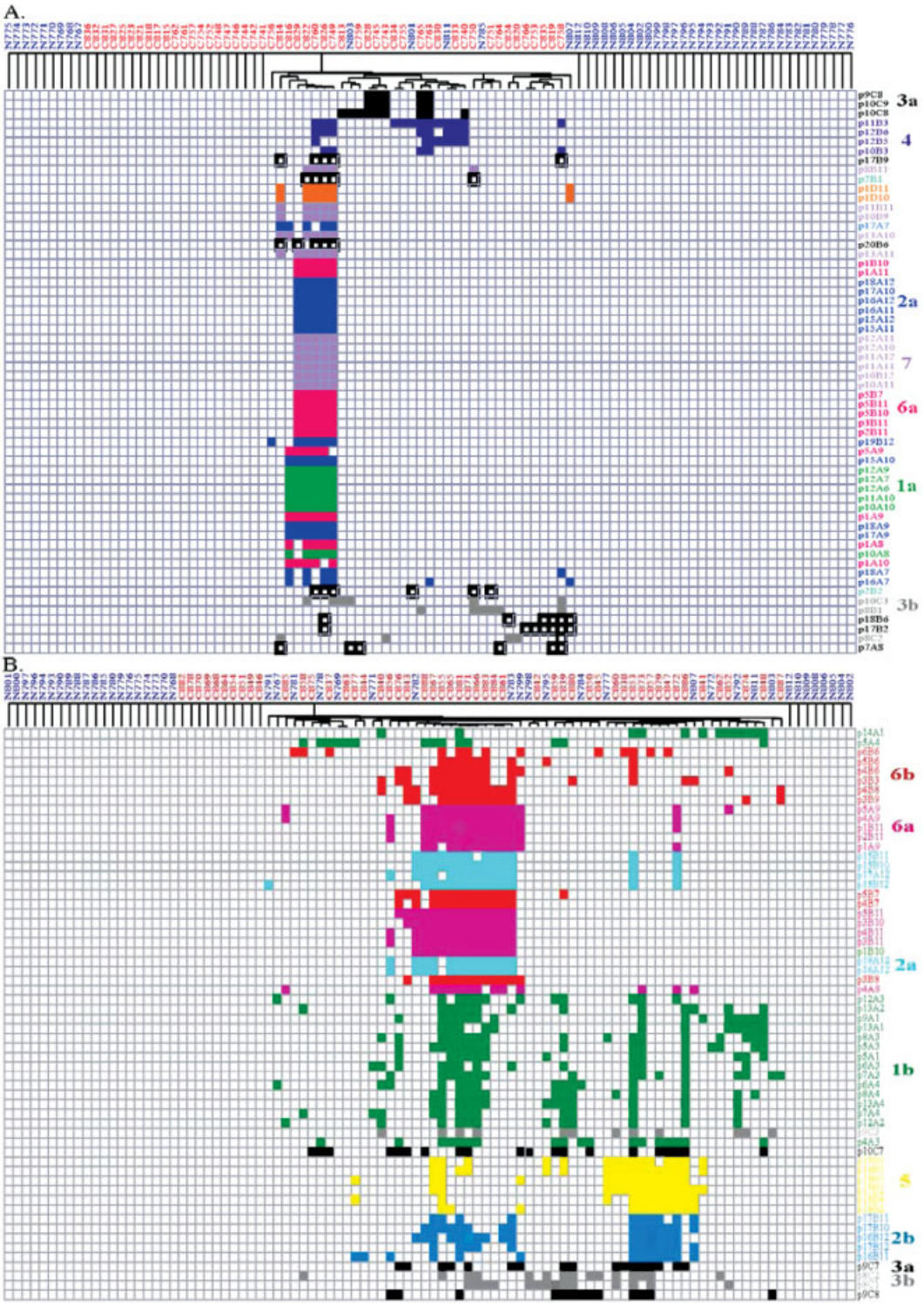

Figure 3. Clusters of fractions and samples. The 60 fractions with the highest M2 scores (from Fig. 2) were clustered (unsupervised average-linked) by reactivity in each sample. Each column represents data from a given sample, and each row is data from a given fraction. The labels of the cancer samples are colored red, and the labels of the control samples are colored blue. The groups of fractions are color-coded and numbered according to the labeling of Fig. 2. A filled-in box indicates a given sample passed the M2 threshold for a given fraction, and a blank box indicates that it did not. (A) Non-organ-confined cancer samples and control samples (from experiment sets one and two). A filled-in box indicates that a sample passed the M2 threshold in both experiment sets for that fraction. (B) Organ-confined cancer samples and control samples (from experiment set three).

tightly-cluster reactivity in one group of the fractionation. Therefore, we reduced our candidate search to proteins that were found in more than one fraction from only one group. Ninety-six proteins from the LTQ-MS/MS analysis and 11 more from the MALDI analysis met these criteria. Each group contained some candidates. When restricting the search to proteins found in three or more fractions from only one group, 21 proteins from the LTQ-MS/MS analysis and one more from the MALDI analysis were found. The protein candidates meeting these criteria are listed in Supporting Table 2.

3.5 Validation using focused protein arrays

Since the highly multiplexed screening method presented above may provide many candidate tumor antigens, it is important to have a complementary method to efficiently test and validate the candidates. We investigated the use of smaller, more focused microarrays of recombinant proteins to validate the immunoreactivity found in the broad screens above. In contrast to the arrays used in the screens, which contained thousands of spots and were printed with one array *per* microscope slide, the focused arrays contained just a few dozen spots each, with 48 arrays printed on each microscope slide. This format allowed the high-throughput analysis of many samples on selected proteins.

The group of fractions with the highest immunoreactivity (group 4 in Fig. 2) was also the smallest group, made up of only four fractions. The hK11 was the only protein identified from that group found in all the fractions analyzed by MALDI-MS/MS but not identified in any other group. Increased expression levels of hK11 were previously associated with prostate cancer [24]. The hK11 was therefore considered one of the strong candidate antigens, and because recombinant versions of the protein were available, we chose it to demonstrate the use of focused arrays for candidate validation.

Focused microarrays containing both isoforms 1 and 2 of this protein were made to test the antibody reactivities to these proteins in 209 serum samples from three patient classes: 66 healthy controls, 70 organ-confined prostate cancer, and 73 non-organ-confined prostate cancer. Incubation of the arrays with anti-human hK11 confirmed the immunoreactivity of the spotted hK11 (Fig. 4A), and a negative control array (no serum) confirmed a lack of nonspecific binding of the detection reagents (Fig. 4B). The incubations of the cancer and control samples (representative images shown in Figs. 4C and D) showed antibody binding to the spotted proteins. Of all the proteins on the array, only hK11 isoform 2 had significantly different ($p<0.05$) binding levels between any of the patient classes. The hK11-reactive antibodies were more prevalent in the cancer patient samples relative to the controls (Fig. 4F). The hK11-reactive antibody levels measured in a repeat experiment using 23 samples showed good agreement with the first set (correlation of 0.87 between sets, data not shown). Receiver-operator character-

Table 2. The 57 fractions that were analyzed by MS[a)]

Section	Fraction	Total identified proteins	Proteins common within section	Proteins unique to section
1	p5A3	3	1	0
1	p4A3	1	1	0
1	p7A3	34	8	2
1	p8A3	18	8	2
1	p12A6	50	1	0
1	p12A7	3	1	0
1	p10A10	3	2	0
1	p11A10	4	2	0
1	p10A11	3	0	0
1	p11A11	1	0	0
2a	p16A7	15	3	0
2a	p17A7	32	24	6
2a	p18A7	53	27	7
2a	p18A9	42	19	6
2a	p15A10	0	0	0
2a	p17A10	11	9	0
2a	p17A9	10	10	4
2a	p18A12	23	7	0
2a	p16A12	5	0	0
2b	p17B10	61	19	4
2b	p17B11	61	18	4
3a	p10C8	11	7	4
3a	p10C9	4	4	2
3a	p9C8	44	13	4
3a	p9C7	46	13	4
3a	p10C7	29	7	4
3b	p9C3	65	13	3
3b	p8C1	31	12	3
3b	p8C2	28	14	6
3b	p8B1	63	3	0
4	p12B5	22	9	3
4	p12B6	13	9	2
4	p12B6*	38	16	8
4	p10B3	25	24	6
4	p10B3*	43	20	11
4	p11B3	19	23	6
4	p11B3*	42	22	11
5	p17B2	62	22	7
5	p18B2	61	22	7
6a	p5A9	2	2	1
6a	p4A9	8	2	1
6a	p4A9*	6	3	1
6a	p4A8	33	2	2
6a	p1A9	3	1	0
6a	p1A10	8	0	0
6a	p1B10	22	3	1
6a	p1B11	2	1	0
6a	p2B11	20	12	2
6a	p3B11	36	22	5
6a	p4B11	38	21	4
6a	p5B11	33	14	3
6b	p3B9	1	0	0
6b	p3B9*	1	0	0
6b	p4B7	46	21	4

Table 2. Continued

Section	Fraction	Total identified proteins	Proteins common within section	Proteins unique to section
6b	p4B8	57	21	4
6b	p3B8	0	0	0
No section	p13A1	0	0	0
No section	p14A1	0	0	0
No section	p12A3	8	0	0
No section	p1D10	9	0	0
No section	p1D11	1	0	0
No section	p12A2	8	0	0

a) The asterisks (*) indicate the fractions that were analyzed by MALDI-MS/MS. All others were analyzed by LTQ-FT-MS. The total number of proteins identified in each fraction is given, followed by the number of proteins in each fraction that were found elsewhere in the group, followed by the proteins found in at least two fractions in a group but not found in any other group (the candidate antigens).

istic analysis showed that hK11-reactive antibodies distinguished between all cancer and the healthy controls with an AUC of 0.84 with a sensitivity of 93% and a specificity of 68% (Fig. 4G).

4 Discussion

We have demonstrated a complete strategy for identifying immunoreactive proteins using natural protein microarrays of cell-line-derived proteins. This strategy included the broad screening of many samples; identifying groups of proteins that contain common immunoreactive proteins; MS identification of the common proteins most likely accounting for the immunoreactivity; and the illustrative validation of a selected protein candidate using focused microarrays of recombinant proteins. Because the instrumentation for producing the proteins and preparing and using the microarrays is relatively straightforward, the technology could be readily adopted in other labs and applied to the study of other diseases that exhibit autoimmunity. Instrumentation for automating 2-D liquid-phase separations is now available, and fractionation services are offered on a contract basis. This approach was effective in identifying groups of fractions with prostate-cancer-associated immunoreactivity and in validating the disease-associated immunoreactivity of hK11.

Several groups of immunoreactive fractions were found. Each group was reactive in up to about 30% of the patients, and about 50% of the patients had reactivity to at least one of the groups. Since the reactivity patterns of the different groups were non-redundant, the proteins responsible for the reactivities potentially could be used together to improve diagnostic performance relative to individual proteins. The testing of additional cell lines and tissues may reveal immunoreactivity in a higher percentage of patients than observed here, which could further advance the diagnostic potential of the method. Another extension of this method would be to use proteins derived from actual tumor tissues, which could more accurately reflect the alterations in tumor proteins in comparison to cell lines. The actual application of a diagnostic device would use purified proteins, rather than chromatography fractions, so these analyses only estimate the eventual diagnostic performance.

An interesting observation from the profiling of the patient sera was the apparently lower level of immunoreactivity in the patients with non-organ-confined cancer, relative to patients with organ-confined cancer. This effect could relate to tumor-induced immunosuppression that allows the cancer to advance [25] or could in some cases simply indicate a weak immune response due to other reasons. Since the levels of tumor-infiltrating lymphocytes can be prognostic for prostate cancer progression [26], it may also be valuable to look at the prognostic value of anti-tumor antibody levels, or the relationship between circulating antibody levels and tumor-infiltrating lymphocyte levels.

The MS analysis of the fractions revealed apparent protein-dependent patterns of resolution, since some proteins were found throughout the fractionation, probably reflecting multiple isoforms, while others were tightly clustered. The tightly clustered proteins were considered better candidates as immunoreactive proteins, as they would be more likely to yield measurable reactivity in one cluster of fractions. That analysis yielded multiple candidate proteins *per* group and highlighted an area for future improvement in the technology. The separations used for this project were not optimized for resolution, as a large amount of protein (50 mg) was loaded onto the first dimension, and the IEF system used here does not have the resolution of the chromatofocusing systems now available [27]. Higher resolution separations, perhaps combined with pre-separation of sub-cellular components, should reduce the complexity to a handful of proteins *per* fraction and simplify the identification of candidate proteins. Another improvement to the method would be better resuspension and spotting of the hydrophobic fractions, which apparently were not resuspended and spotted because of the aqueous buffer used. Buffers containing organic solvents could be used just for those fractions, so long as the solvents do not interfere with the microarray analysis. The hydrophobic proteins could be important in tumor antigen studies, because membrane-bound proteins, especially those on the cell surface, can be important in the aberrant function and antigenicity of tumor cells.

Focused microarrays were effective for testing and validating a candidate protein. This type of array provides a complementary follow-up to broad screening arrays. The validation of immunoreactivity using focused microarrays was illustrated with the protein hK11. The hK11 (also known as hippostatin) is a member of the kallikrein family of secreted serine proteases, which includes PSA (hK3). In

previous work, hK11 mRNA was found to be over-expressed in 43/66 (65%) of prostate cancer tissue samples [28], and isoform 2 protein was shown to have an increased abundance in the serum of 60% of men with prostate cancer compared with normal [24]. Over-expression in the tumor environment could be responsible for the generation of an immune response against the protein, as observed in this work. We only observed immunoreactivity against isoform 2 (known as the prostate type), and not isoform 1 (brain type), which may indicate that only isoform 2 is over-expressed in the tumor, consistent with their previously observed tissue specificities.

One of the limitations of the focused-array validation method is the need for recombinant proteins. Since the emphasis of this work was advancing the technology and better characterizing the overall immunoreactivity of prostate cancer, we demonstrated the focused array approach on a candidate for which recombinant versions were readily available.

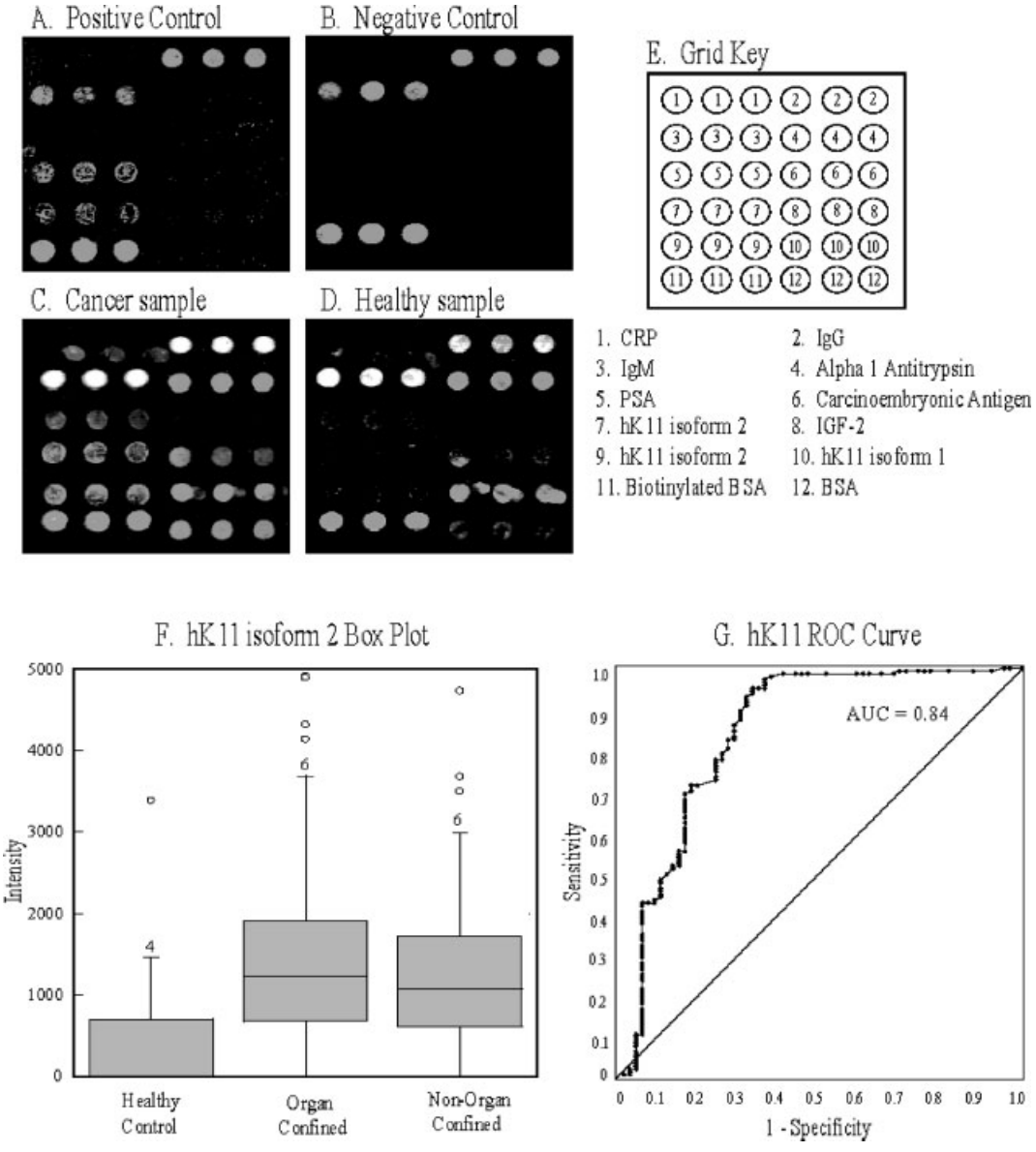

Figure 4. Microarray screening of hK11 immunoreactivity. Microarrays were printed with the pattern given in (E). Representative images are given of incubations with (A) the positive control anti-hK11 antibody; (B) buffer; (C) serum from a cancer patient; and (D) serum from a control subject. The brightness of each spot indicates the level of antibody binding to that spot, and white pixels indicate saturation of detector response. (F) Distributions of the reactivity with hK11 isoform 2 in the indicated sample classes. The box indicates the upper and lower quartiles, the horizontal line the median, and the vertical lines the range. The numbers above each box indicate the number of outliers for each class. (G) Receiver-operator characteristic curve analysis of hK11 isoform 2 in distinguishing all prostate cancer patient samples from the control samples.

Other proteins identified by MS/MS were good candidates for further study, based on their previous associations with prostate cancer or cancers in general. Our future validation studies will focus on proteins identified in fresh experiments with the new methods of separation suggested above, since those new methods will provide more precise leads on the candidate proteins. In order to study future candidates efficiently, it may be valuable to have a high-throughput protein expression system, for example using on-chip translation of selected sequences [29]. However, immunoreactivity may only be present in proteins taken directly from cell lines or tumor tissue, so it may be necessary to use proteins purified from those materials.

In summary, this work has demonstrated an effective strategy for profiling patterns of immunoreactivity and for identifying tumor antigens using natural protein microarrays. We used the method to reveal distinct patterns of immunoreactivity against multiple proteins in prostate cancer patients, and focused microarrays of candidate proteins, which complemented the larger, screening arrays, were useful for validating immunoreactivity against the protein hK11. This work lays the groundwork for the broader application of this method for biomarkers of prostate cancer and other cancers.

We thank Paul Norton, Pete Haak, and Dr. James Resau for the protein microarray printing at the VAI Molecular Diagnostics Laboratory. We gratefully acknowledge grant support from the Michigan Economic Development Corporation (GR356, GR887), the Early Detection Research Network, NIH/NCI grant 2U01CA8632306, and additional support from the Van Andel Research Institute.

5 References

[1] Bouwman, K., Qiu, J., Zhou, H., Schotanus, M. *et al.*, *Proteomics* 2003, *3*, 2200–2207.

[2] Yan, F., Sreekumar, A., Laxman, B., Chinnaiyan, A. M. *et al.*, *Proteomics* 2003, *3*, 1228–1235.

[3] Sahin, U., Tureci, O., Schmitt, H., Cochlovius, B. *et al.*, *Proc. Natl. Acad. Sci. USA* 1995, *92*, 11810–11813.

[4] Sahin, U., Tureci, O., Pfreundschuh, M., *Curr. Opin. Immunol.* 1997, *9*, 709–716.

[5] Scanlan, M. J., Welt, S., Gordon, C. M., Chen, Y. T. *et al.*, *Cancer Res.* 2002, *62*, 4041–4047.

[6] Huang, S., Preuss, K. D., Xie, X., Regitz, E., Pfreundschuh, M., *Cancer Immunol. Immunother.* 2002, *51*, 655–662.

[7] Wang, X., Yu, J., Sreekumar, A., Varambally, S. *et al.*, *N. Engl. J. Med.* 2005, *353*, 1224–1235.

[8] Hong, S. H., Misek, D. E., Wang, H., Puravs, E. *et al.*, *Cancer Res.* 2004, *64*, 5504–5510.

[9] Brichory, F. M., Misek, D. E., Yim, A. M., Krause, M. C. *et al.*, *Proc. Natl. Acad. Sci. USA* 2001, *98*, 9824–9829.

[10] Brichory, F., Beer, D., Le Naour, F., Giordano, T., Hanash, S., *Cancer Res.* 2001, *61*, 7908–7912.

[11] Le Naour, F., Misek, D. E., Krause, M. C., Deneux, L. *et al.*, *Clin. Cancer Res.* 2001, *7*, 3328–3335.

[12] Nam, M. J., Madoz-Gurpide, J., Wang, H., Lescure, P. *et al.*, *Proteomics* 2003, *3*, 2108–2115.

[13] Le Naour, F., Brichory, F., Misek, D. E., Brechot, C. *et al.*, *Mol. Cell. Proteomics* 2002, *1*, 197–203.

[14] Chinni, S. R., Falchetto, R., Gercel-Taylor, C., Shabanowitz, J. *et al.*, *Clin. Cancer Res.* 1997, *3*, 1557–1564.

[15] Sreekumar, A., Laxman, B., Rhodes, D. R., Bhagavathula, S. *et al.*, *J. Natl. Cancer Inst.* 2004, *96*, 834–843.

[16] Ogata, R., Matsueda, S., Yao, A., Noguchi, M. *et al.*, *Prostate* 2004, *60*, 273–281.

[17] McNeel, D. G., Nguyen, L. D., Storer, B. E., Vessella, R. *et al.*, *J. Urol.* 2000, *164*, 1825–1829.

[18] Nilsson, B. O., Carlsson, L., Larsson, A., Ronquist, G., *Ups. J. Med. Sci.* 2001, *106*, 43–49.

[19] Daniels, T., Zhang, J., Gutierrez, I., Elliot, M. L. *et al.*, *Prostate* 2005, *62*, 14–26.

[20] Shi, F. D., Zhang, J. Y., Liu, D., Rearden, A. *et al.*, *Prostate* 2005, *63*, 252–258.

[21] Schena, M., Shalon, D., Davis, R. W., Brown, P. O., *Science* 1995, *270*, 467–470.

[22] Qiu, J., Madoz-Gurpide, J., Misek, D. E., Kuick, R. *et al.*, *J. Proteome Res.* 2004, *3*, 261–267.

[23] Chen, S., Haab, B. B., in Van Eyk, J., Dunn, M. (Eds.), *Clinical Proteomics*, Wiley-VCH, Weinheim, Germany 2007.

[24] Diamandis, E. P., Okui, A., Mitsui, S., Luo, L. Y. *et al.*, *Cancer Res.* 2002, *62*, 295–300.

[25] Burnet, F. M., *Prog. Exp. Tumor Res.* 1970, *13*, 1–27.

[26] Vesalainen, S., Lipponen, P., Talja, M., Syrjanen, K., *Eur. J. Cancer* 1994, *30A*, 1797–1803.

[27] Zhu, Y., Lubman, D. M., *Electrophoresis* 2004, *25*, 949–958.

[28] Stavropoulou, P., Gregorakis, A. K., Plebani, M., Scorilas, A., *Clin. Chim. Acta* 2005, *357*, 190–195.

[29] Ramachandran, N., Hainsworth, E., Bhullar, B., Eisenstein, S. *et al.*, *Science* 2004, *305*, 86–90.

